

Investigation on the drop break-up under controlled mixed shear and elongational flow conditions in combination with the morphology and rheology of emulsifiers at the drop's interface

**Peter Fischer, Stefan F. M. Kaufmann, Nicole Maag, Kentaro Maruyama,
Carsten Cramer, Erich J. Windhab**

**Swiss Federal Institute of Technology Zürich (ETH Zürich)
Institute of Food Science, Laboratory of Food Process Engineering
ETH Zentrum, Universitätsstrasse 2, CH-8092 Zürich, Switzerland
E-mail: peter.fischer@ilw.argl.ethz.ch**

Abstract

Large variety of multiphase systems is treated in dispersing operations in order to generate a well defined disperse microstructure. Beside material properties as viscosity and interfacial tension, the ratio of shear and elongational forces in the flow field is of importance. In this paper we focus on the deformation and disruption of droplets in specially designed flow cells that allows to control the flow stresses acting on the droplets. The presents of surfactants or emulsifiers at the interface of the droplets influence the deformation and eventually the break-up of the aggregates. To study the quiescent and transient rheology and morphology of such interfacial films and the resulting drop properties Brewster angle microscopy and interfacial rheometry are used. The obtained information on the structure and rheology provides insight into molecular and organization at the interface and, therefore on emulsification processes.

Keywords: Deformable interfaces, interfacial rheology, mixed flow fields, surfactants, Brewster Angle Microscopy

Introduction

The flow of fluids composed of immiscible liquide-liquid mixtures is of interest in a wide range of research fields, such as foods, polymers, pharmaceuticals and cosmetics. The controlled manufacturing of the size and shape of liquid-liquid mixtures is one of the major goals in multiphase fluid research. In general, small droplets are generated in dispersing processes where big aggregates are deformed and broken up in flow fields. The deformation and breakup behavior is influenced mainly by stresses acting in the flow and the material behavior of the dispersed and continuous phases, as well as by the interface properties. The stresses which act on single droplets come from three main sources: flow, interfacial tension and Brownian forces where only the first both are considered in the following. Stresses due to flow depend on the flow field characteristics and on the rheology of the fluid phases while stresses due to the interface also depend on the rheology of the fluid phases, as well as on added surfactants. General qualitative relationships have been found between these three stress sources and some structural characteristics of emulsions in an equilibrium state. To produce and stabilize such products amphiphilic molecules, i.e. emulsificators (emulsions, microemulsions, multiple emulsions and suspension) or compatilizers (polymer blends, composites) are used. By adding such surface acting components one is potentially able to alter the physical and chemical properties (viscosity,

elasticity, surface tension, phase behavior, domain structures) of the interfaces in defined ways. For the stability, performance and quality of multiphase products the interfacial film, its structure, interfacial tension and rheological properties are considered to be strongly relevant. In particular, the rheology of the interfacial film has a significant influence on emulsifications, emulsion stability, foam stability and de-foaming. Focussing on liquid-liquid interfaces (droplets) the manifold interaction among interfacial rheology, interfacial structure together with flow stresses acting on the deformable soft surfaces, time-dependent concentration gradients in planar (e.g. Marangoni effect) and three dimensional phases, transport phenomena, and adsorption kinetics are of interest. To date, precise quantitative and qualitative information about this influence is limited.

Deformation and break-up of single drops in under shear and elongational flow fields

It is known that droplet deformation and break-up in elongational flow fields is much more efficient compared to pure shear flows. These conditions are locally fulfilled in a Four-Roll Mill as shown in Fig. (1).



Figure 1: Four-Roll Mill.

In previous experimental work we focused on the deformation and disruption of microscopically small “naked” droplets in specially designed flow cells as band-shear apparatus, tube apparatus, four-roll mill, and eccentric cylinders that allow controlled shear and elongational flow fields and therefore controlled stress acting on the droplets to be deformed and eventually dispersed. The deformation and dispersion of droplets are recorded with a CCD camera to the computer as digital data. In Fig. (2) the drop deformation in the stagnation flow domain of the Four-Roll Mill under mixed shear and elongational flow conditions is demonstrated [1, 2]. The elongated filament eventually breaks up and generates very narrowly size-distributed droplets. To describe the droplet deformation and breakup, at least in the equilibrium (Fig. 3a) the viscosity of the dispersed, η_d , the continuous fluid phases, η_c , and the interfacial tension, σ or σ^* are used.

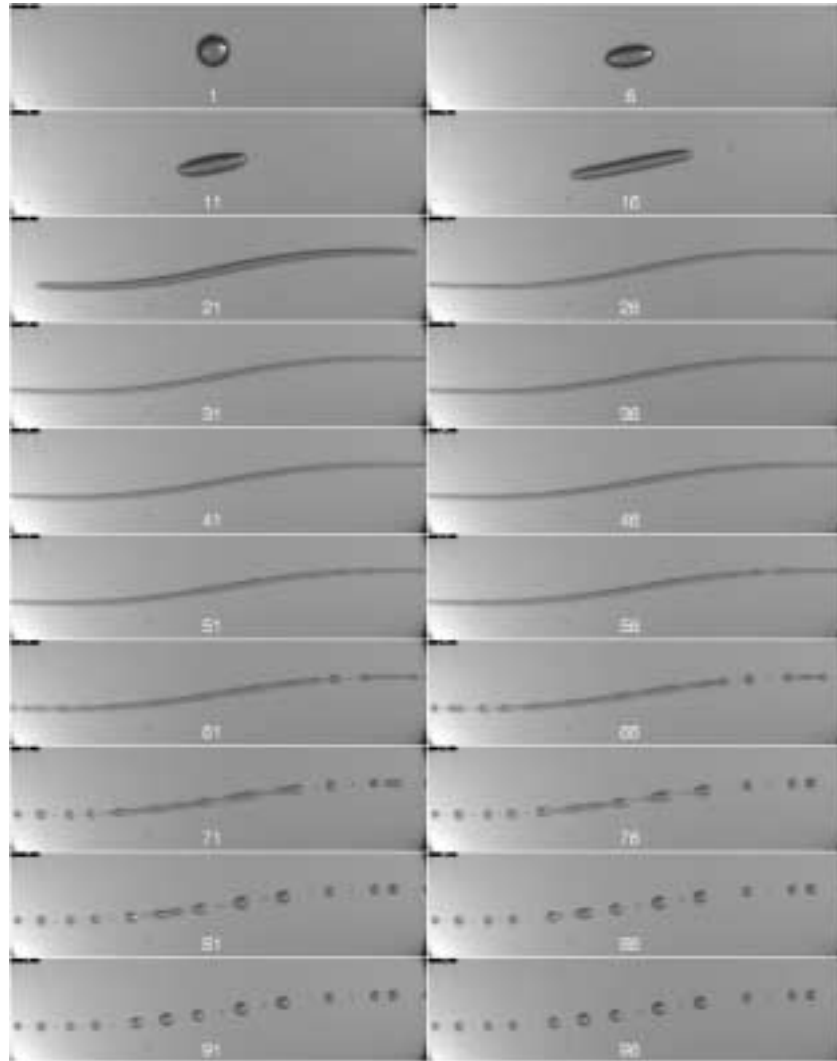


Figure 2: Deformation of a drop and, consequently, structural changes of a drop interface in mixed shear and elongational flow (PEG in silicon oil AK 5000).

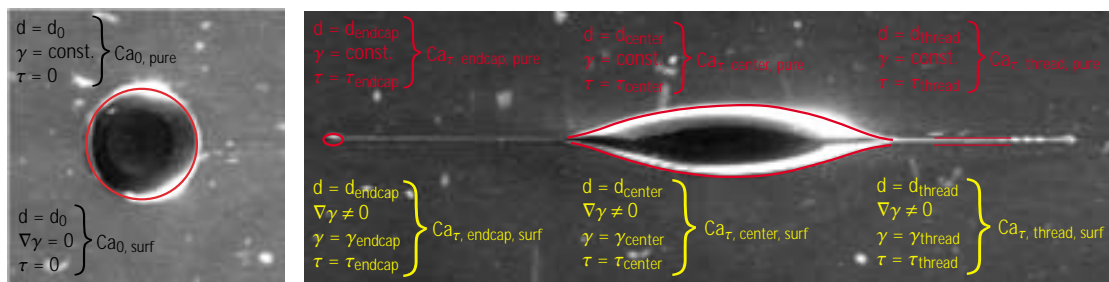


Figure 3: a.) Undisturbed and b.) Disturbed drop and the resulting changes in physical properties.

As dimensionless parameters, the Capillary number, Ca , displays the ratio of viscous forces, which work to deform the drop, to interfacial tension, which works to restore the shape of the drop by

$$Ca = \frac{\text{viscous forces}}{\text{interface forces}} = \frac{\tau d}{\sigma} = \frac{\eta_c \dot{\gamma} d}{\sigma} \quad \text{Eq. (1)}$$

where d is the radius of the undeformed drop, τ the shear stress, and $\dot{\gamma}$ is the local shear

rate. Once the flow, i.e. deforming stresses beginning to act on the droplet several assumptions as constant d , η_c , σ , and even constant $\dot{\gamma}$ as given in Eq. (1) do not apply. Depending on the deformed shape of the droplet as shown in Fig. (3b) one may identify several different Ca numbers depending on the diameter of the droplet's parts (center, thread, endcap). A detailed description of the velocity field can be received from flow visualization experiments and from Computational Fluid Dynamics (CFD) that provide data of the flow parameters such as elongational rate and shear stress, etc. [3, 4].

Interfacial assemblies, their interfacial rheology and structure

In industrial processes, surfactants are often added to emulsions to stabilize them against droplet coalescence. The presents of surfactants or emulsifiers at the interface of the droplets influence the deformation and eventually the break-up of the aggregates. When surfactants are present, variations in interfacial tension arise since there are gradients in surfactant concentration along the interface as the droplet deforms. Additionally the surfactant is transported along the interface toward the tips of the drop as shown in Fig. (4).

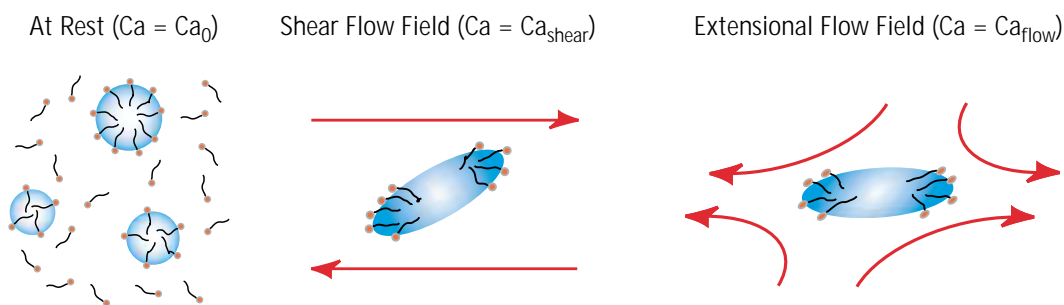


Fig. 4: Distribution of surfactants at the interface in rest and in shear and extensional flow conditions.

This produces surfactant concentration gradient, and consequently changes in the interfacial tension σ [5, 6]. The variations in interfacial tension change the balance of interfacial stress tangentially through Marangoni stresses. In most experimental and theoretical approaches σ is taken to be constant, so that Marangoni stresses are neglected. For nonsoluble monolayers at the air/water interface the mechanical and rheological properties and the state of aggregation (diffusivity, viscosity, elasticity) of monolayers can be modified through compression. For liquid-liquid phase boundary one may consider a similar approach as long as a “nonsoluble” surfactant is confined to the interface and is not able to move in either of the both bulk phases. The relationship between the interfacial tension and the local surface excess concentration of surfactant is referred to as the equation of state for the interfacial tension. For dilute surfactant concentrations at rest one obtains

$$\sigma^* = \sigma(1 - \beta\Gamma) = \sigma \frac{1 - \beta\Gamma}{1 - \beta} \quad \text{with} \quad \beta = \frac{\Gamma_0 RT}{\sigma_s} \quad \text{Eq. (2)}$$

where σ^* is the interfacial tension of the covered interface, σ the interfacial tension of the “clean” interface, Γ the surfactant concentration at the drop's interface. Once the system shows dynamic interfacial effects as interfacial tension gradients one has to introduce Γ_0 as reference concentration of the initial state, i.e. the interface at rest or an undeformed

drop. In the case of higher concentration of the surfactant one will observe surfactants also in one or both bulk phases. The interfacial coverage then is mainly controlled by adsorption and desorption of molecules, i.e. surfactant excess in the bulk and not any longer by diffusion/forces movement of surfactant molecules along the interface due to concentration gradients or flow of the bulk phases. As a consequence, distinguish phases and concentration gradients as shown in Fig. (5a) are not present but a dense surface coverage and solved molecules in the bulk phases can be observed as shown in Fig. (5b).

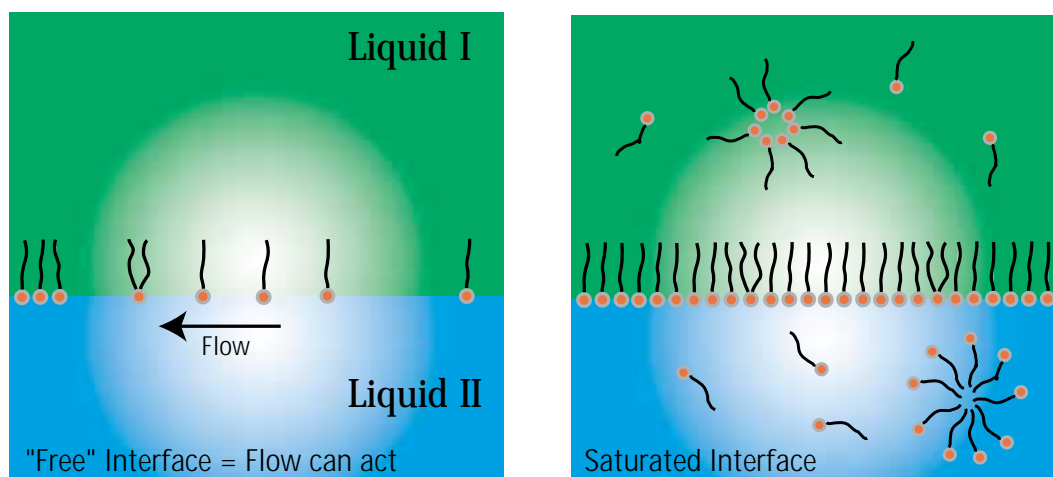


Figure 5: Aggregation of "nonsoluble" surfactant at the liquid-liquid interface. a.) External stresses and thermodynamics allow flow in the interface. b.) External flow has little effect on saturated interface.

Since the concentration of the surfactant is deterring the aggregation of the layer and flow induced concentration change also will be reflected in a change of interfacial rheology (viscosity and elasticity of the interface).

Rheomorphological behavior of the phase boundary

A interfacial rheometry was used to investigate the interfacial rheology of cellulose monolayer while structural properties were simultaneously be investigated by BAM (Fig. 6) [7-9].

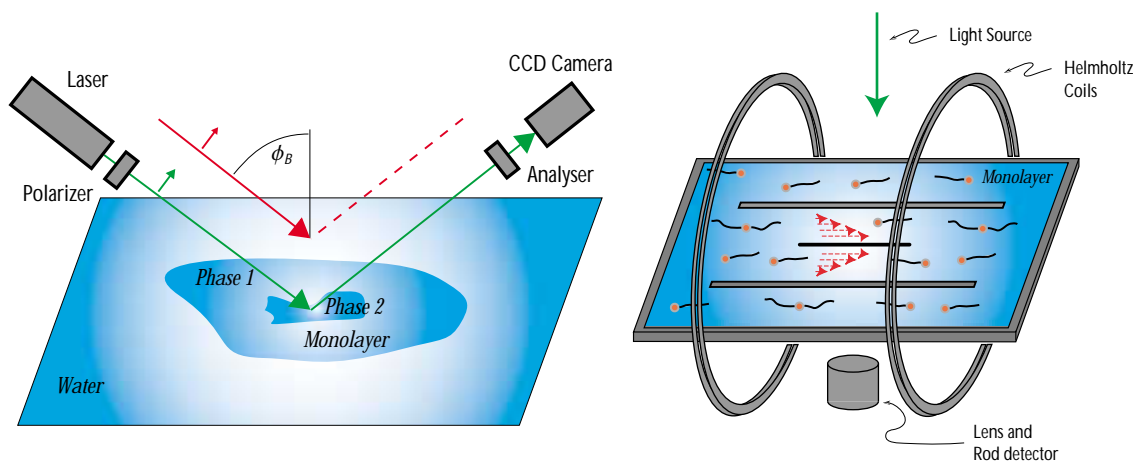


Fig. 6: BAM studies under flow and surface rheological measurements in shear flow.

Within this study BAM images and surface rheological measurements indicate significant

changes in morphology as shown in Fig. (7) and monolayer mechanical properties during compression.

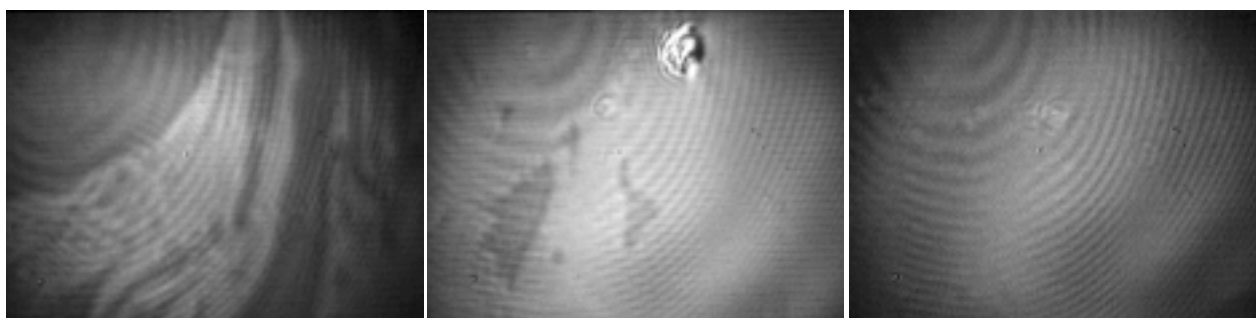


Figure 7: BAM images recorded for spread monolayers of HPC-C18 at different surface pressures (vertical length of all images is 1mm).

Importantly, these changes can be correlated with each other and the isotherm shape. The results, in general, are interpreted as a complex indication of the partial crystallization of interdigitated sidechains, made possible by bilayer formation. From the results we were able to deduced a Rheo-Morphological Phase Diagram, represented by the loss angle, $\tan \delta = G_S''/G_S'$, as plotted in Fig. (8). The rheological properties of the HPC-C18 monolayer exhibit a strong temperature dependence.

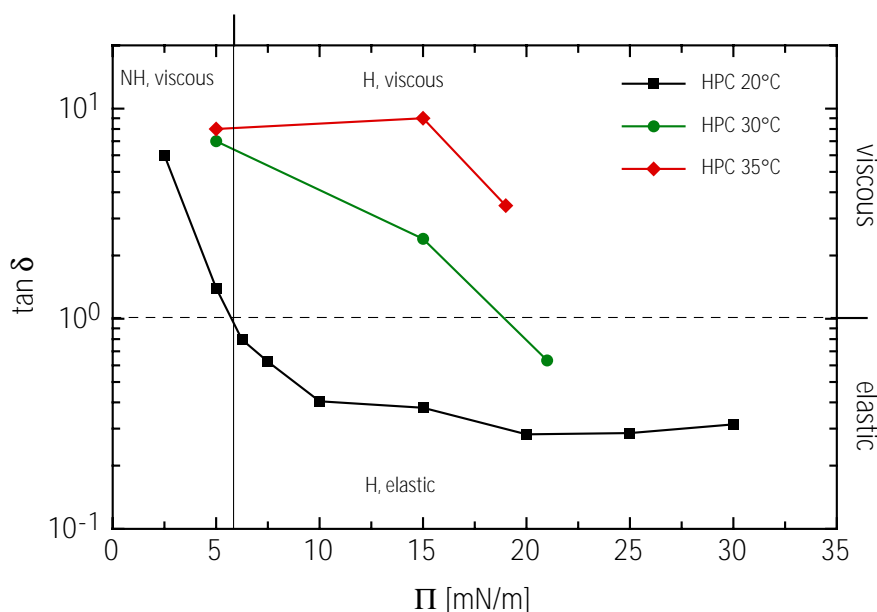


Figure 8: Rheo morphological phase diagram (represented by $\tan \delta$) as a function of the surface pressure for HPC-C18. Divisions between phases are indicated by a vertical and horizontal lines.

Summary

In summary, it is shown that in well-defined shear and/or elongational dispersing flow fields the microstructure can be adjusted in order to generate specific rheological and quality properties of the resulting product. It is also demonstrated how the synergistic application of dispersing flow experiments and Computational Fluid Dynamics (CFD) allow to understand and eventually optimize dispersing flow processes and related product properties. To study the rheology and morphology of liquid-liquid interfacial films and the

resulting drop properties two techniques as Brewster Angle Microscopy and interfacial rheometry were used. The interaction among interfacial rheology and interfacial structure are given by time-dependent concentration gradients, transport phenomena, adsorption kinetics, and "extra" shear and extensional stresses that can induce additional anisotropic orientation and organization of the interface under flow and may influence the drop deformation and break-up. In summary, knowledge of the structural and rheological can provide insight into molecular interactions and organization at the interface and, therefore on emulsification processes.

Literature

- [1] Beeler T: Optische Untersuchungen von Einzeltropfen im Vierrollenapparat, Semesterarbeit supervised by P. Fischer, ETH Zürich, Zürich, Switzerland (1999).
- [2] N. Maag: Untersuchungen von Tropfendispergiervorgängen in Scher- und Dehnströmungsfeldern unter Verwendung eines Vierrollenapparat, Diplomarbeit supervised by S. Kaufmann, ETH Zürich, Zürich, Switzerland (1999).
- [3] Kaufmann S, Fischer P, Windhab E: Investigation of droplet dispersing processes in shear and elongational flow, in Proceedings of the Second International Symposium of Food Rheology and Structure edited by P. Fischer; I. Marti and E. Windhab, Zurich, Switzerland, (2000).
- [4] K. Maruyama, P. Fischer, E. Windhab: Investigation on the droplet breakup in mixed shear and elongational flow conditions, PGS autumn meeting, Aarau, Switzerland, (2000).
- [5] Edwards, D. A.; Brenner, H.; Wasan, D. T. Interfacial Transport Processes and Rheology; Butterworth-Heinemann: Boston, 1991
- [6] H.A. Stone, A simple derivation of the time-dependent convection-diffusion equation for surfactant transport along a deforming interface, Phys. Fluids A 2 (1990) 111-112.
- [7] Fischer P, Brooks CF, Fuller GG, Ritcey AM, Xiao Y, Rahem T: Phase behavior and flow properties of "Hairy-rod" monolayers, Langmuir 16 (2000) 726.
- [8] Fischer P: Investigation of rheological and structural properties of interfaces by Brewster-Angle Microscopy and interfacial rheology, in Proceedings of the Second International Symposium of Food Rheology and Structure edited by P. Fischer; I. Marti and E. Windhab, Zurich, Switzerland, (2000).
- [9] D. Hönig, G.A. Overbeck, D. Möbius: Morphology of pentadecanoic acid monolayers at the air/water interface studied by BAM, Adv. Mater. 4 (1992) 419.